Supporting Information for

Anion-dependent assembly of Dy complexes: structures and magnetic behaviors

Peng Chen,*[ab] Meiqi Zhang,[a] Wenbin Sun,[a] Hongfeng Li,[a] Lang Zhao[b] and Pengfei Yan*[a]

[a] Key Laboratory of Functional Inorganic Material Chemistry (MOE), School of Chemistry and Materials Science, Heilongjiang University, Harbin 150080, PR China. E-mail address: jehugu@gmail.com (Chen P.); yanpf@vip.sina.com (Yan P.)

[b] State Key Laboratory of Rare Earth Resource Utilization, Changchun Institute of Applied Chemistry, Chinese Academy of Sciences, Changchun 130022, China.

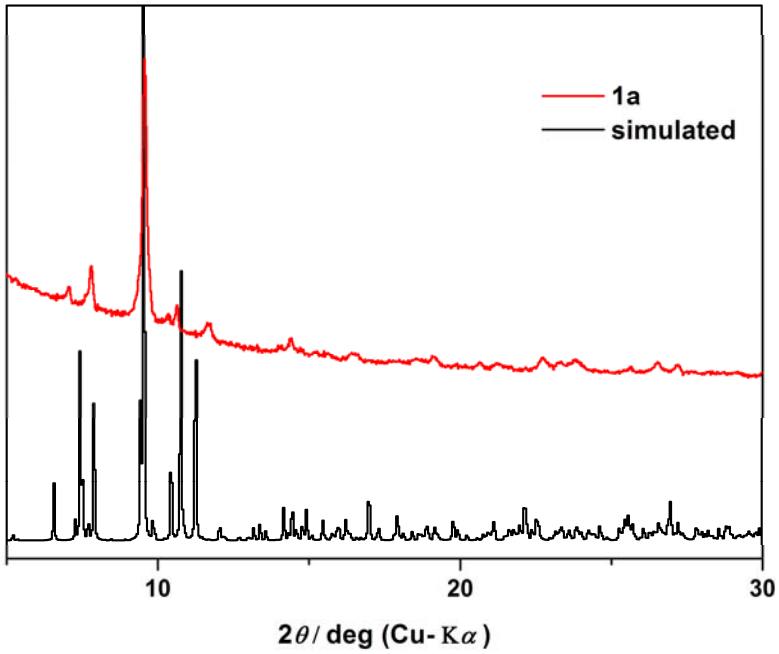

Figure S1 Simulated and experimental Xrd patterns of **1a**.

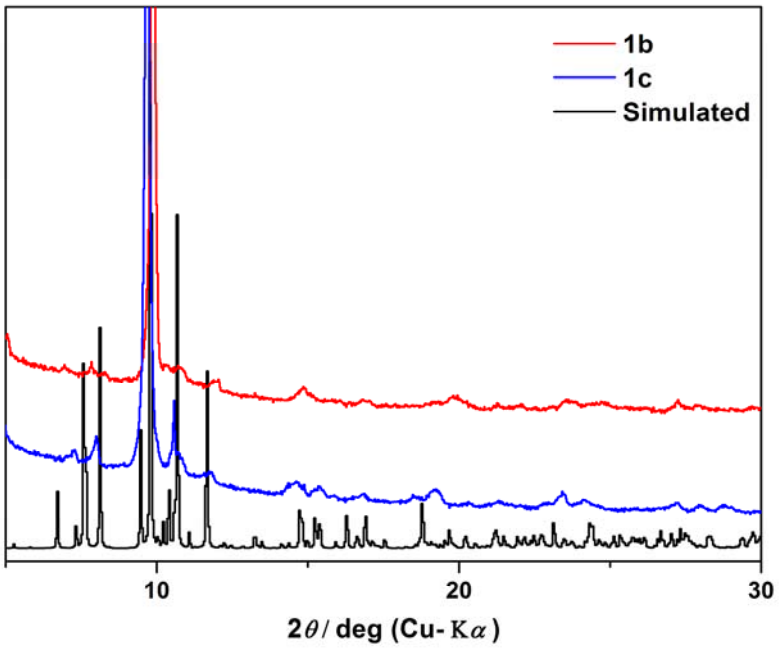

Figure S2 Simulated and experimental Xrd patterns of **1b** and **1c**.

1a−**1c** are supposed to be sensitive to the air that the single crystal analyses were performed at 150 K under N_2 atmosphere. And their structures collapse on desolvation, when powder X-ray analyses are performed.

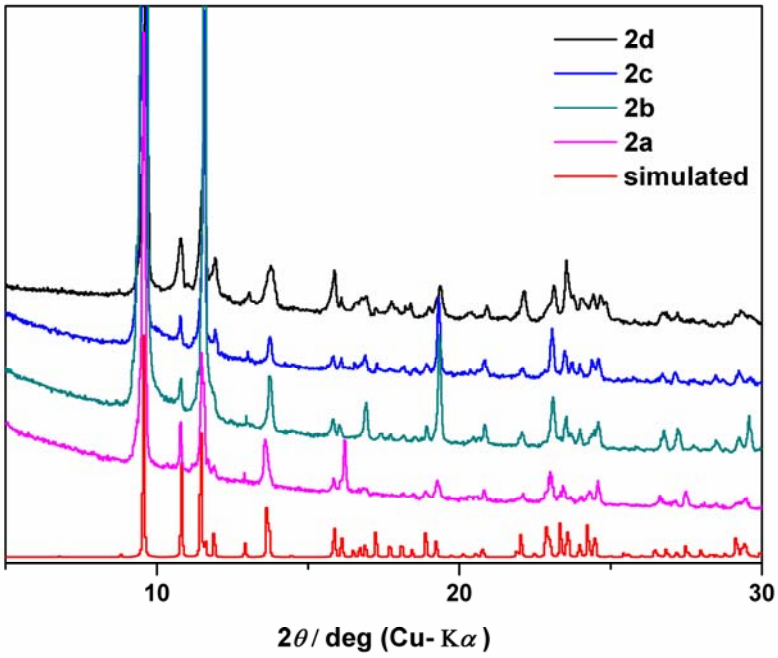

Figure S3 Simulated and experimental Xrd patterns of **2a**−**2d**.

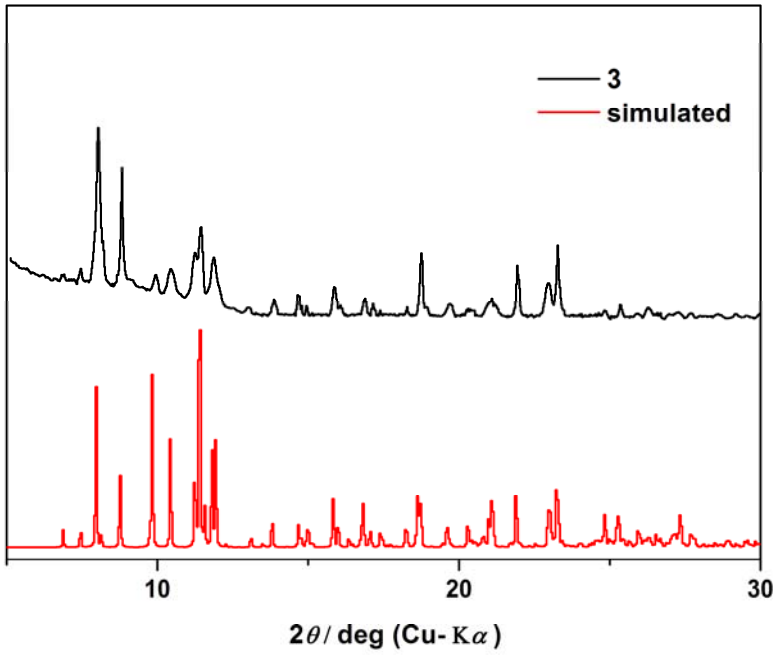

Figure S4 Simulated and experimental Xrd patterns of **3**.

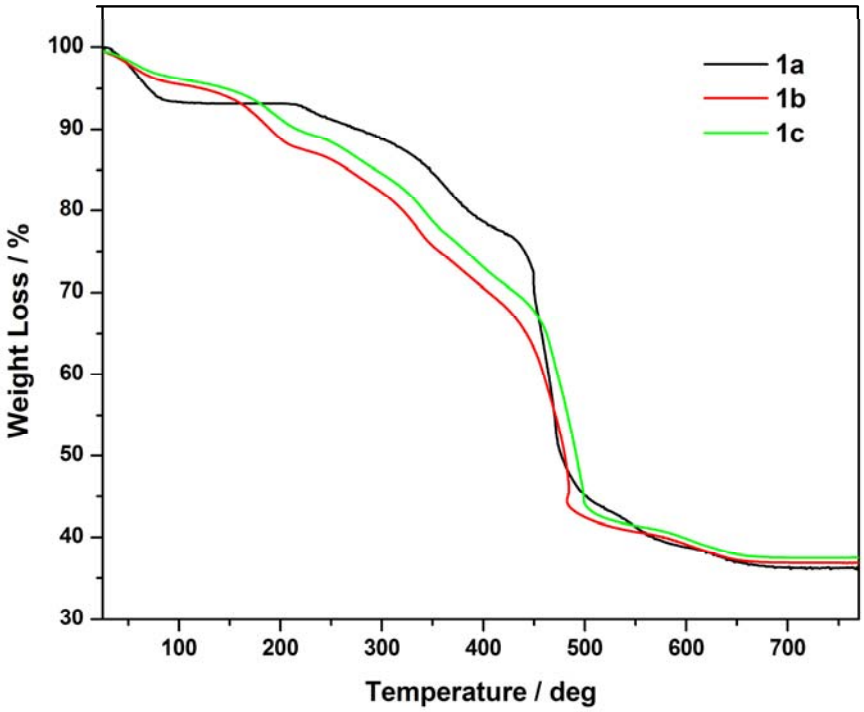

Figure S5 TG curves of **1a**, **1b** and **1c**.

TG analysis indicates a total weight loss of 63.88 wt% (calcd. 65.94 wt%) for **1a**. The first stage is ascribed to the loss of methanol and hydrate molecules until 100 ^{o}C (found 6.82 wt%, calcd. 7.08 wt%). And the second stage occurring at 220 ^{o}C until 430 ^{o}C is owing to the removal of one ligand (found 17.3 wt%, calcd. 17.90 wt%). However, it is hard to distinguish each other that the loss of the second ligand of and decomposition of the acetates might be a continuous process. Around 470 ^{o}C, the acetates start to decompose. For the case of **1b** and **1c**, it is evident that their stability is much poorer than **1a**, and the ligand starts to decompose around 100 ^{o}C. However, similar temperature range has been observed for the removal of second ligand and acetates as **1a**. In all, a total weight loss of 61.88 wt% and 61.42 wt% (calcd. 63.04 wt% and 62.59 wt%) are found for **1b** and **1c**, respectively.

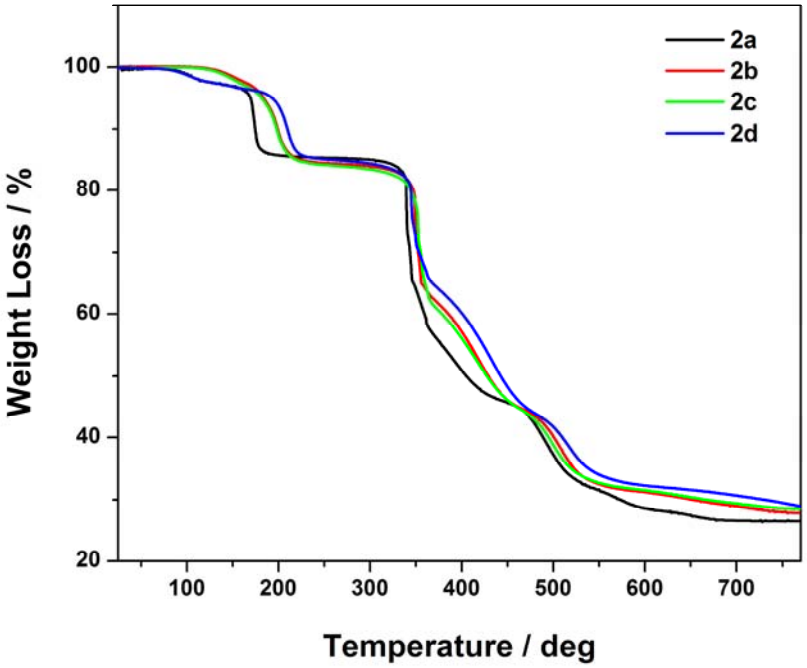

Figure S6 TG curves of **2a**–**2d**.

TG analyses indicate a total weight loss of 73.48, 72.16, 71.50 and 71.05 wt% (calcd. 73.86, 72.22, 71.83 and 71.32 wt%) for **2a**–**2d** in the experimental range, respectively. The first stage is mainly ascribed to the loss of methanol molecules around 190 ^{o}C, and the second stage is owing to the removal of DMSO molecules until 300 ^{o}C. For the first two stages, a total weight loss of 15.01, 16.92, 16.61 and 15.67 wt% is found (calcd. 17.12, 16.73, 16.64 and 16.52 wt %), respectively. Then, further weight loss (~40 wt%) is detected until ~480 ^{o}C, which is corresponding to the decomposition of the ligand (calcd. 41.21, 40.29, 40.08 and 39.79 wt%). Finally, the rest weight loss is believed to the removal of nitrate groups until the end of the experiments.

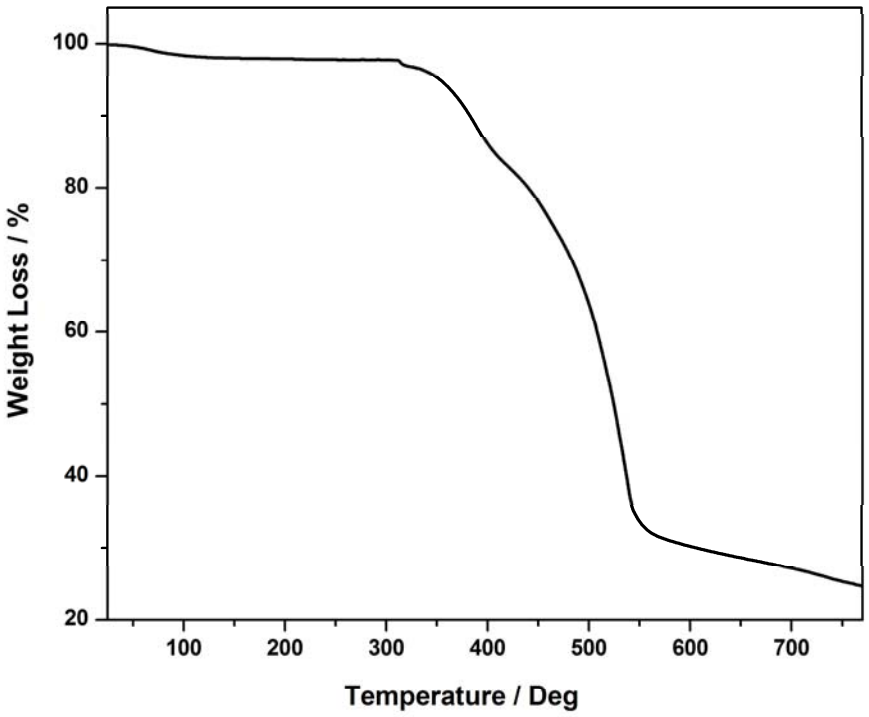

Figure S7 TG curve of **3**.

TG analysis indicates a total weight loss of 65.30 wt% (calcd. 66.94 wt%) for **3**. In the first stage, the loss of methanol is found until 100 ^{o}C (1.87 wt%, calcd. 1.98 wt%). Then, the main weight loss is attributed to the removal of the ligand (calcd. 65.62 wt%), and the third stage is owing to the decomposition of perchloride (calcd. 10.34 wt%). The removal of the ligand and perchloride might be a continuous process that it is not possible to clearly distinguish them. Unfortunately, we can not measure it at higher experimental temperature due to the limitation of the equipment.

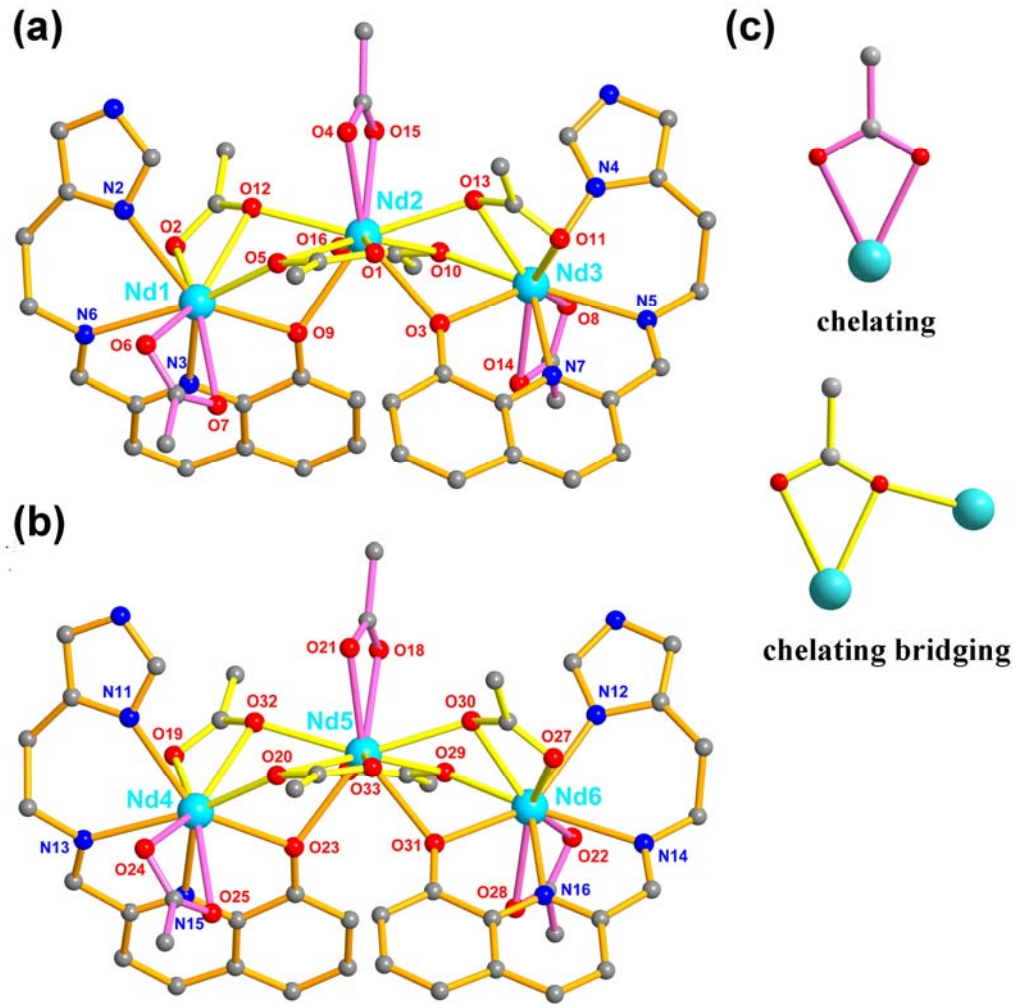

Figure S8 Partially labeled units containing Nd1 (a) and Nd4 (b) ions in **1a** (Hydrogen atoms have been omitted for clarity); (c) coordination modes found for acetates in **1a**.

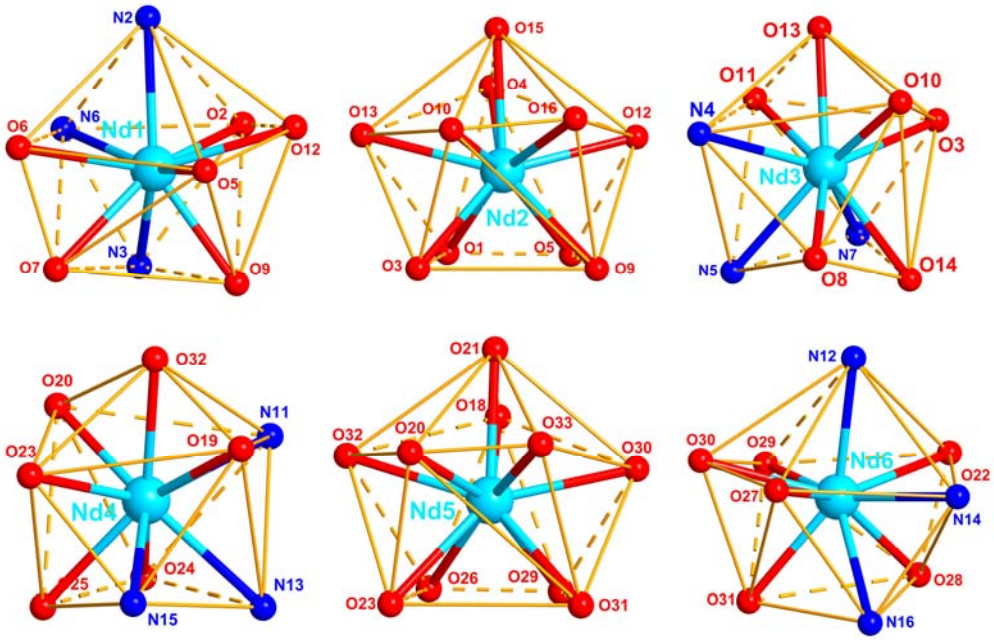

Figure S9 Coordination geometry of Dy^{3+} ions in **1a**

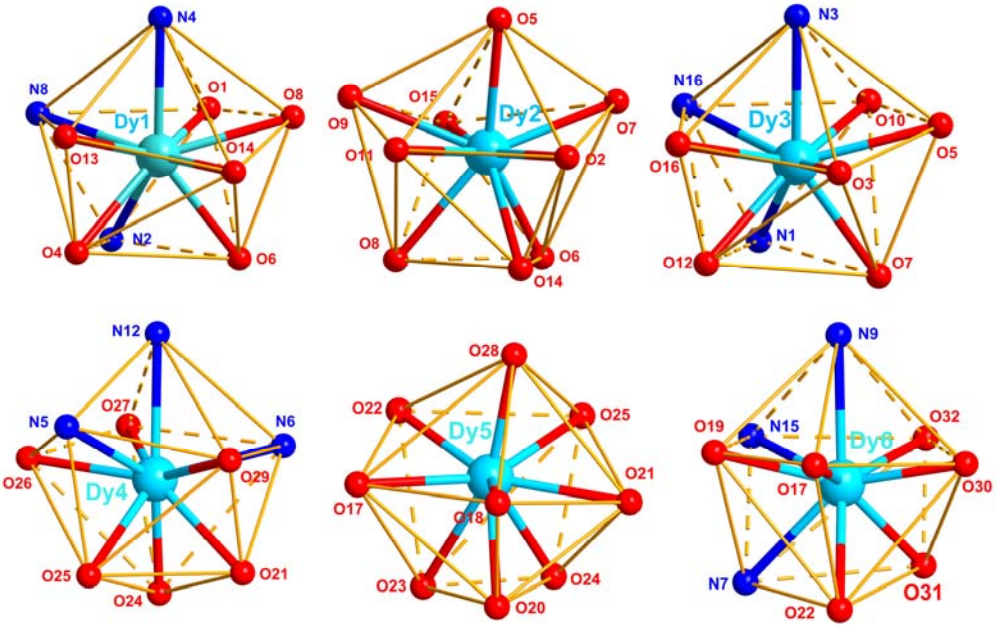

Figure S10 Coordination geometry of Dy^{3+} ions in **1c**

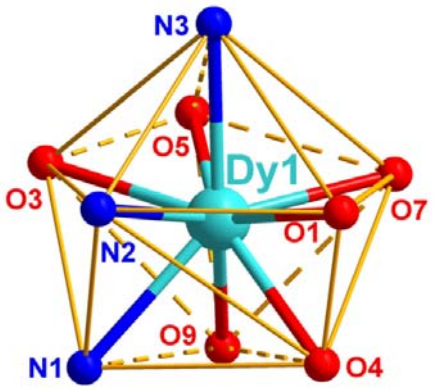

Figure S11 Coordination geometry of Dy^{3+} ions in **2c**

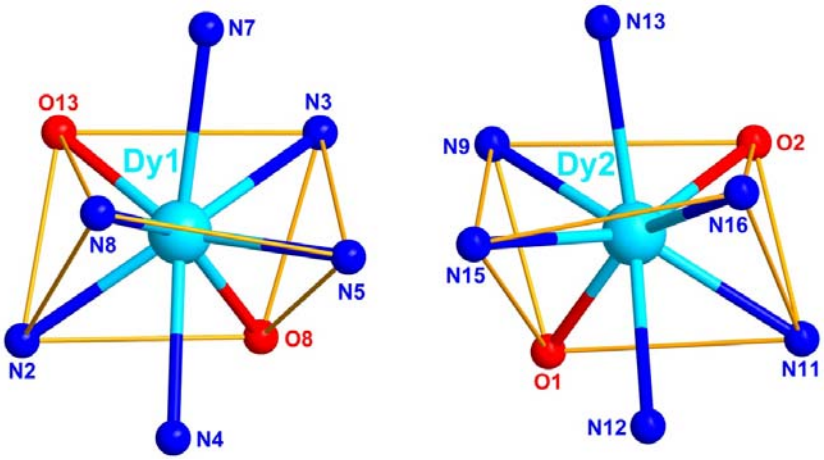

Figure S12 Coordination geometry of Dy^{3+} ions in **3**

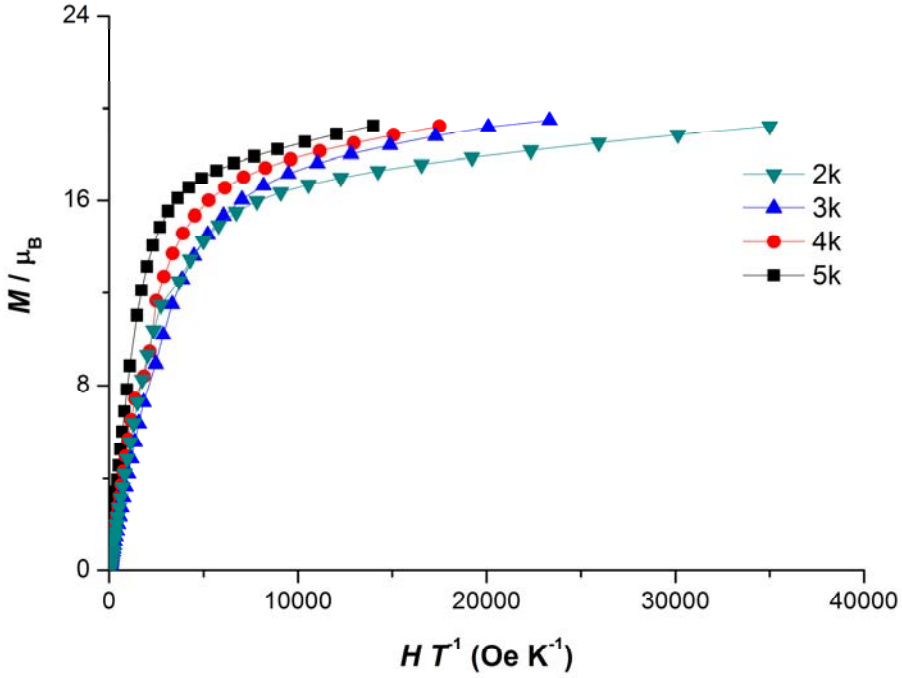

Figure S13 *M vs. H/T* plot at the indicated temperature for **1c**.

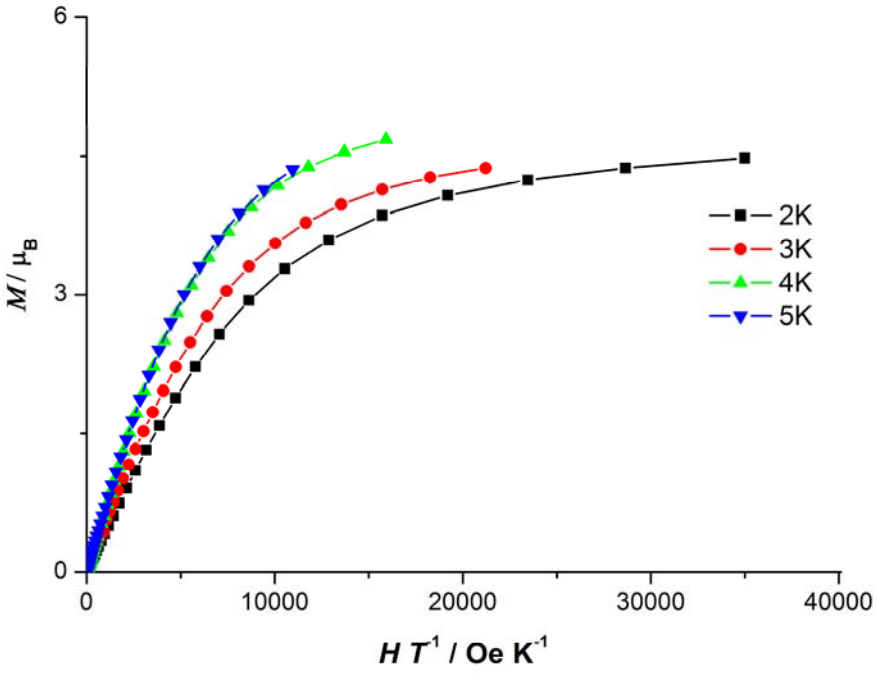

Figure S14 *M vs. H/T* plot at the indicated temperature for **2c**.

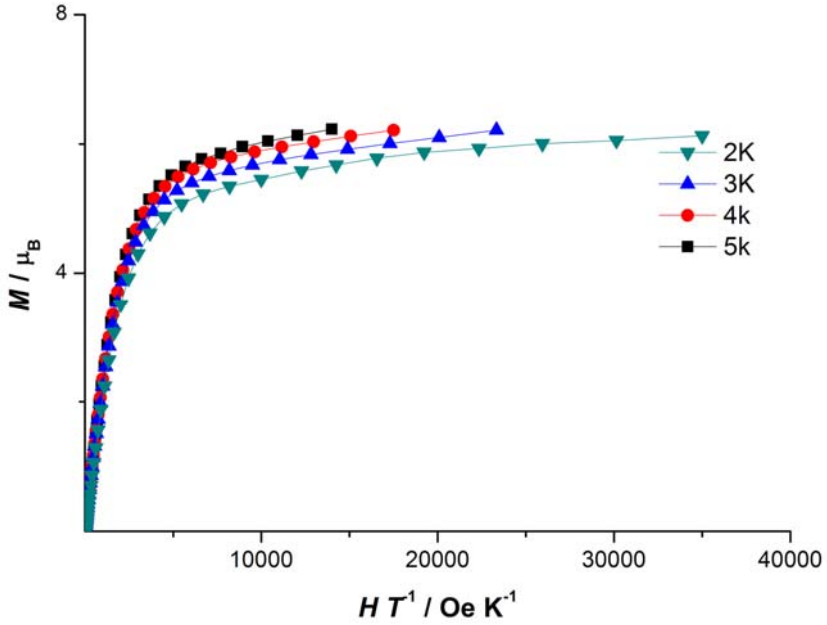

Figure S15 *M vs. H/T* plot at the indicated temperature for **3**.

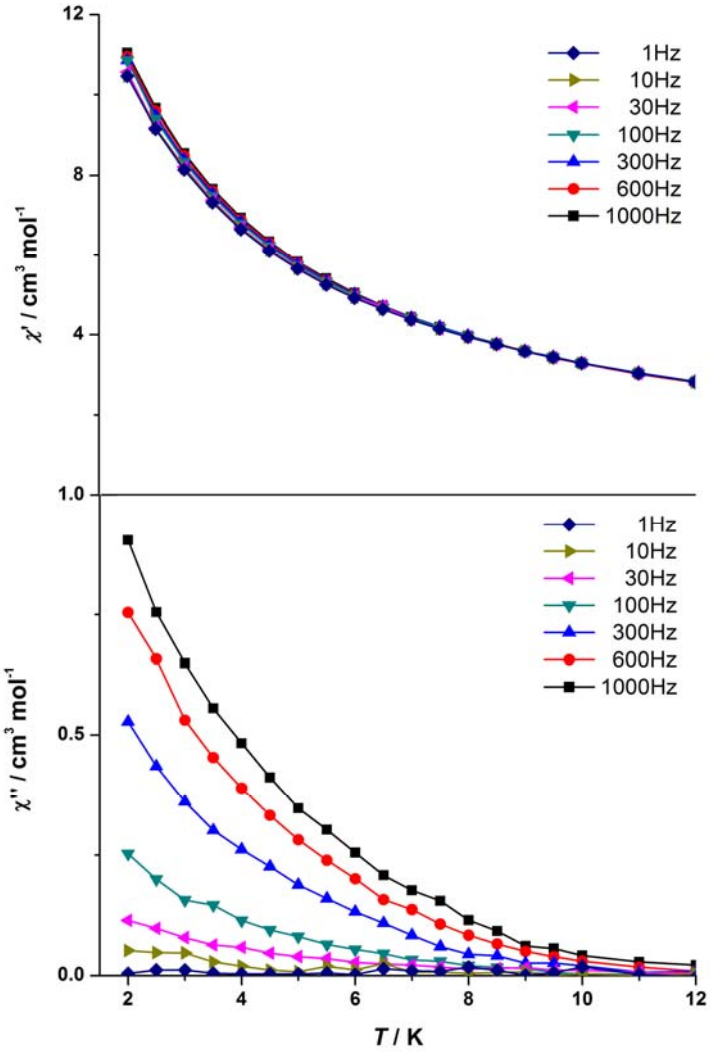

Figure S16 Temperature dependence of in-phase and out-of-phase ac susceptibility of **1c** under zero dc field.

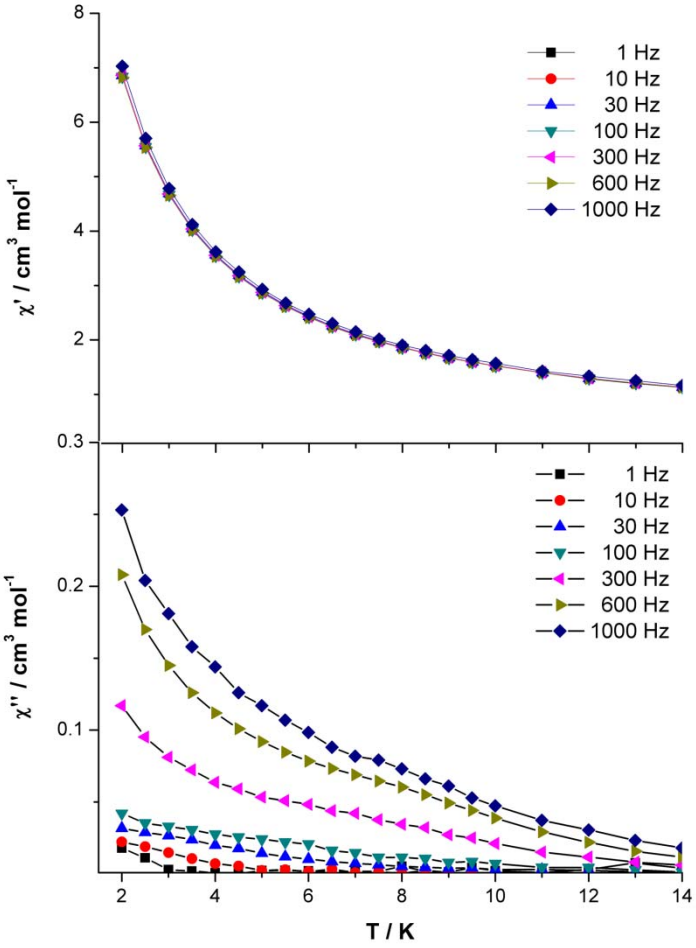

Figure S17 Temperature dependence of in-phase and out-of-phase ac susceptibility of **2c** under zero dc field.

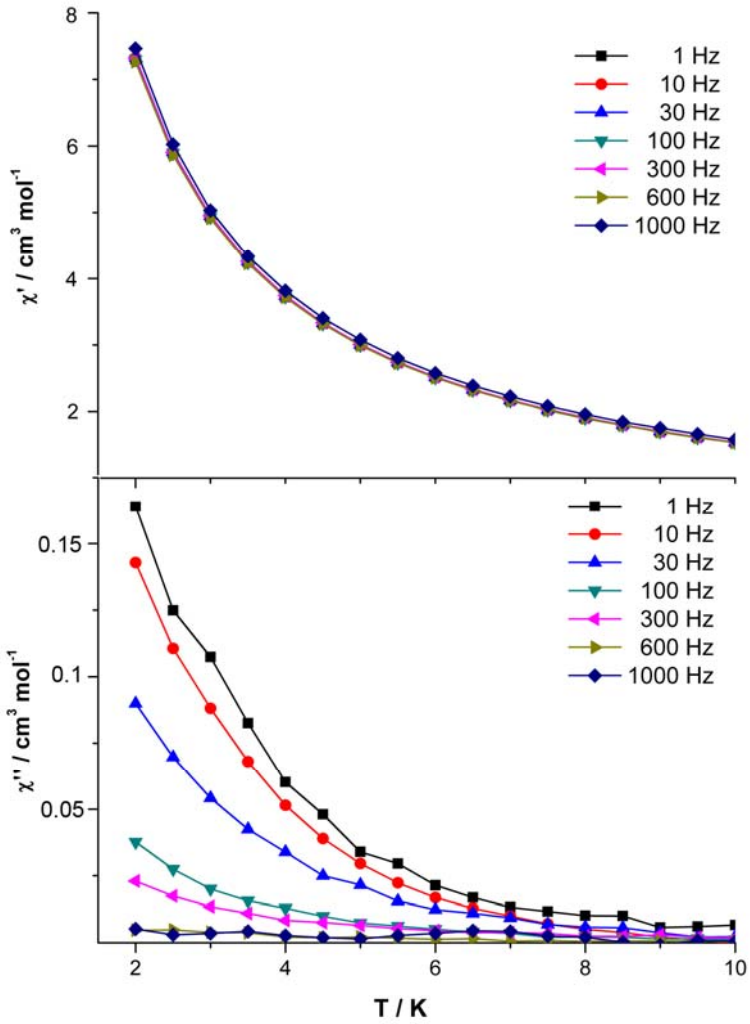

Figure S18 Temperature dependence of in-phase and out-of-phase ac susceptibility of **3** under zero dc field.

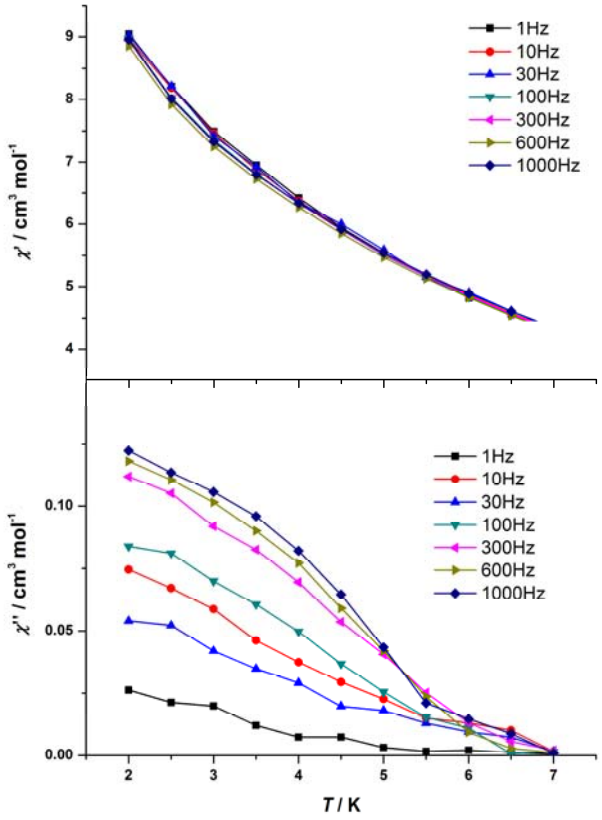

Figure S19 Temperature dependence of in-phase and out-of-phase ac susceptibility of **1c** under applied dc field of 2000 Oe.

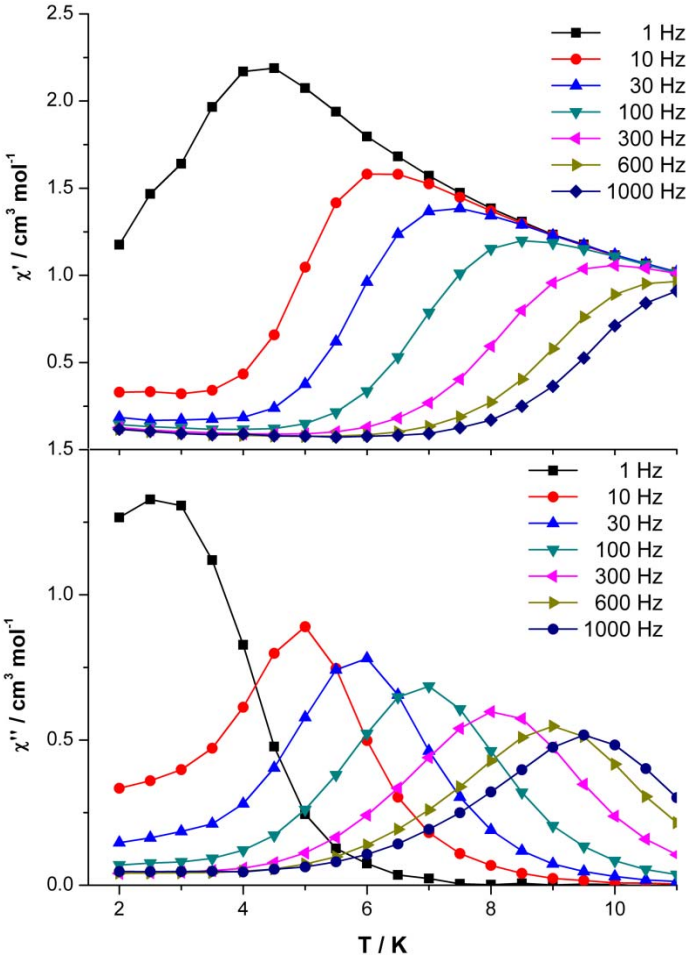

Figure S20 Temperature dependence of in-phase and out-of-phase ac susceptibility of **2c** under applied dc field of 2000 Oe.

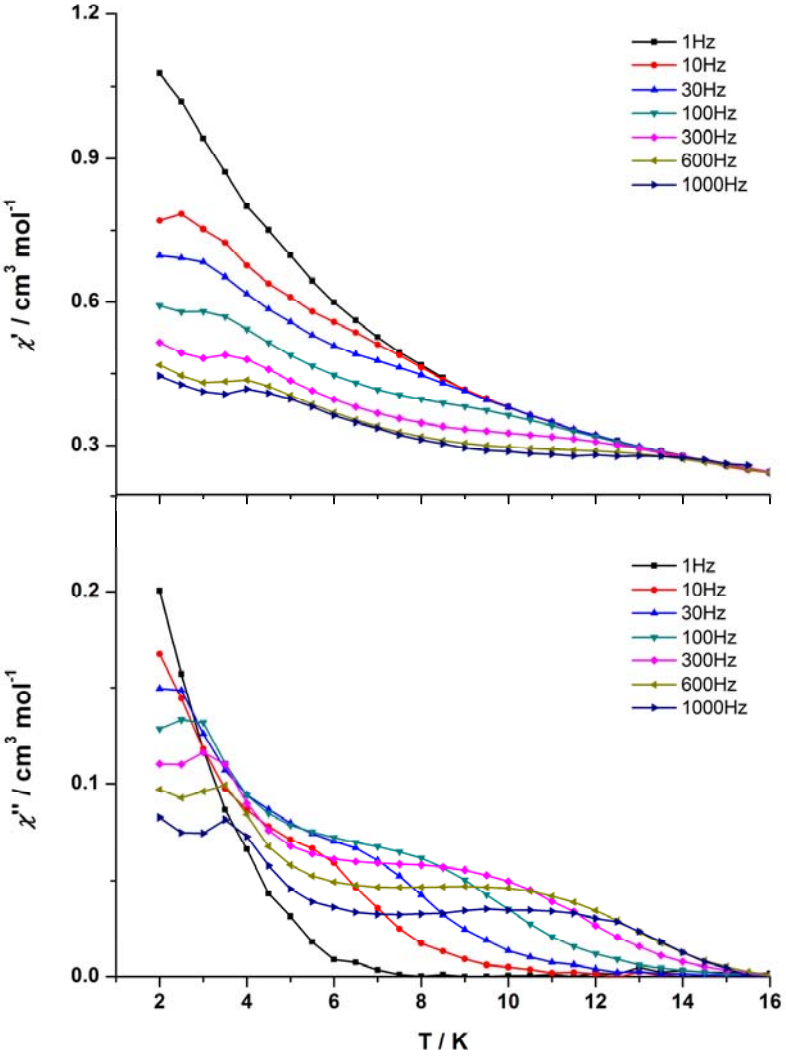

Figure S21 Temperature dependence of in-phase and out-of-phase ac susceptibility of **3** under applied dc field of 2000 Oe.

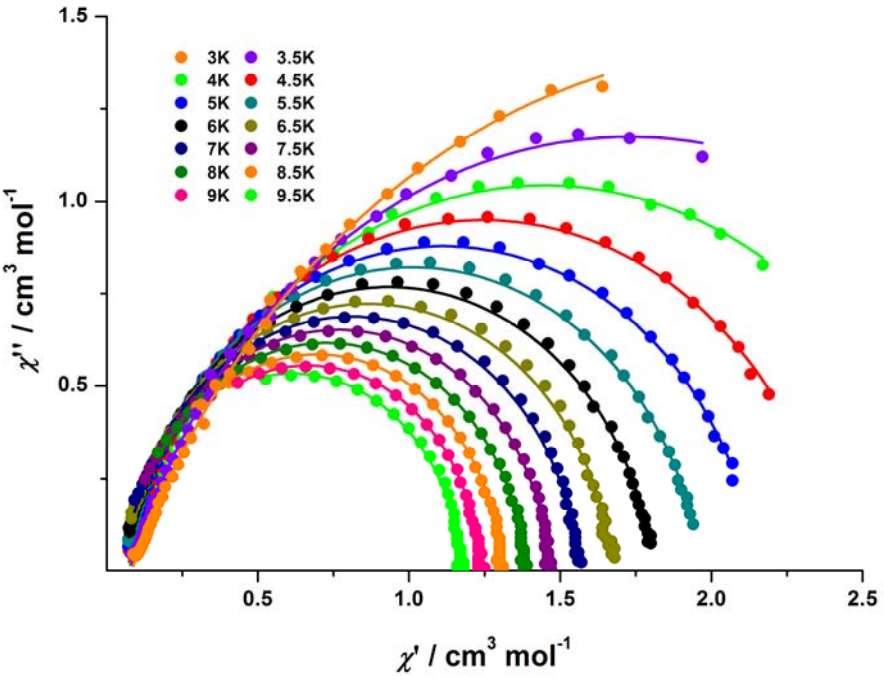

Figure S22 Cole–Cole plot of **2c** at the indicated temperature

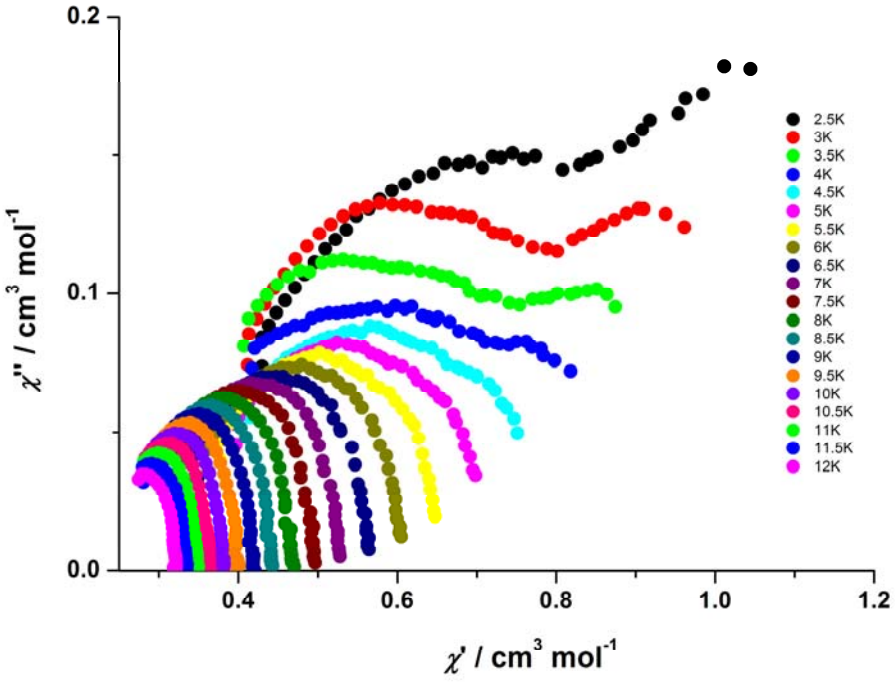

Figure S23 Cole–Cole plot of **3** at the indicated temperature

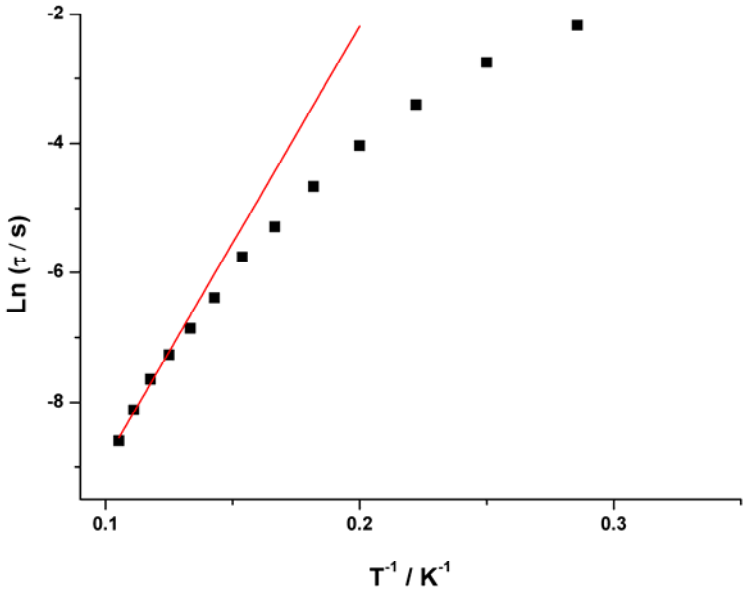

Figure S24 Magnetization relaxation time, *τ, versus* T^{-1} plot for **2c** under an applied dc field of 2000 Oe

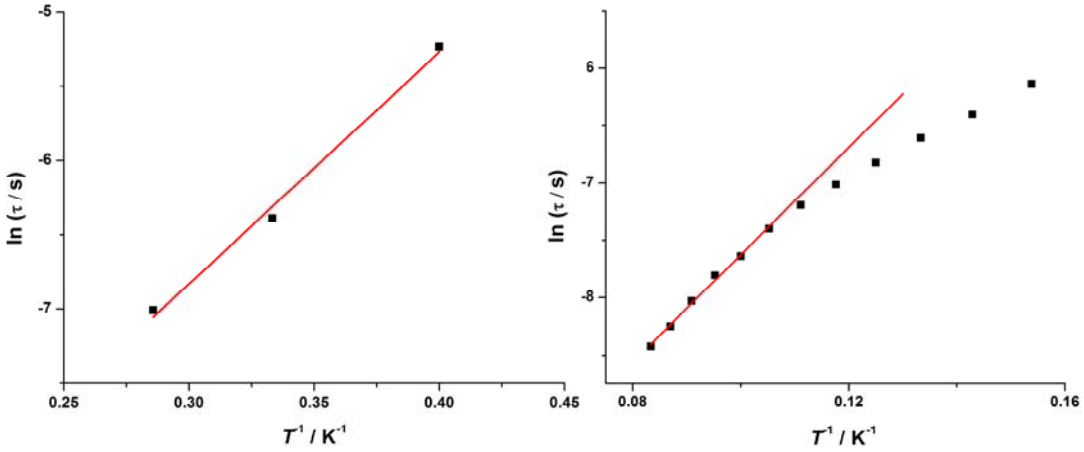

Figure S25 Magnetization relaxation time, *τ, versus* T^{-1} plot (left, low temperature domain; right, high temperature domain) for **3** under an applied dc field of 2000 Oe